TSUNAMI SIMULATIONS OFF THE WEST COAST OF SUMATRA USING DISPERSIVE AND NON-DISPERSIVE WAVES

Dwi Hartanto[*] **Supervisor: Tatsuhiko SAITO**[**]
MEE11620 **Yushiro FUJII**[***]

ABSTRACT

To reduce future tsunami hazards, tsunami simulations for possible future events in the Mentawai region, especially the Padang area, based on dispersive wave equations (DSP) and non-dispersive wave equations, namely liner long-wave (LLW) and non-linear long-wave (NLLW), were conducted in this research. Through these simulations we attempted to estimate maximum tsunami height and tsunami arrival time for the Padang area assuming probable scenarios for future events. An additional objective was to understand which dispersive and non-linear terms affect the tsunami simulation results.

The simulation results were categorized into two parts. For deep water we compared DSP with LLW, and for shallow water, NLLW with LLW. From these comparisons we found that in deep water DSP almost similar with LLW; dispersive waves appear when a station is located perpendicular to the fault strike. Comparison of difference depth of 5, 10, and 20 km in the DSP simulations for scenario earthquake of Mw 8.5 shows that dispersive wave appears more clear at shallow depth. This indicates that dispersive wave may be useful for judging whether earthquake rupture reaches very shallow part near the trench or the rupture occurs only in deep part. In shallow water, advection and bottom friction terms should be considered when the depth is less than 50 m. Our simulations produced a maximum tsunami height in the Padang area of 0.91, 2.02 and 5.65 m for scenario earthquake of Mw 8.1, 8.5 and 8.9. The tsunami arrival times was 24, 20 and 17 min, for the scenarios of Mw 8.1, 8.5 and 8.9, respectively. In the Padang area tsunami countermeasures should be increased for the future earthquakes.

Keywords: Tsunami simulation, dispersive wave, maximum tsunami height, tsunami arrival time, Mentawai, Padang area.

1. INTRODUCTION

After the megathrust earthquakes in Aceh on December 26, 2004 and Nias on March 28, 2005 the next megathrust earthquake is predicted to occur in the Mentawai region (Natawidjaja, 2007). The last megathrust earthquake in the Mentawai region were in 1797 (Mw 8.4) and 1833 (Mw 8.9) (Natawidjaja *et al.*, 2006).

The Bengkulu earthquake (Mw 8.4) on September 12, 2007 and the Mentawai earthquake (Mw 7.7) on October 25, 2010 both occurred in the area of the Mentawai megathrust (Figure 1). This

[*] Meteorology Climatology and Geophysics Agency (BMKG), Jakarta, Indonesia.
[**] National Research Institute for Earth Science and Disaster Prevention (NIED), Tsukuba, Japan.
[***] International Institute of Seismology and Earthquake Engineering (IISEE), Building Research Institute (BRI) Tsukuba, Japan.

two earthquakes reduced the energy that is stored in the Mentawai region, however, much energy is still stored and will be released in the future. The rupture area of the 2010 Mentawai earthquake and 2007 Bengkulu earthquake is only 1/3 of the 1797 and 1833 earthquakes.

If we plot the data from USGS and Global CMT (1973 - May 2012), it shows that to the west of Padang there is a seismic gap (Figure 1). The purpose of this study is to estimate the maximum tsunami height and tsunami arrival time in Padang area using probable scenarios for future events. Also we attempted to find how influential dispersive wave (DSP) and non-linear effects would be to the simulations, by comparing DSP with linear long-wave (LLW) for deep water, and non-linear long-wave (NLLW) with LLW for shallow water.

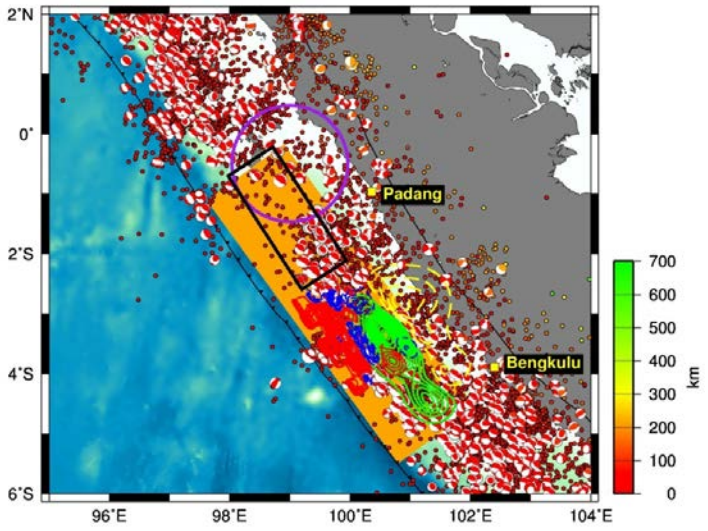

Figure 1. The rupture areas of the 1833 earthquake (orange rectangle) modified from the figure by Newman *et al.*, (2011). Red (uplift) and blue (subsidence) contours are seafloor deformation from the 2010 Mentawai earthquake (Satake *et al.*, 2012), with a contour interval of 0.1 m. Green (uplift) and yellow (subsidence) contours are seafloor deformation from 10-subfault model of the 2007 Bengkulu earthquake (Fujii and Satake, 2008), with a contour interval of 0.2 m. Purple circle indicates a seismic gap near Padang. The figure also includes assumed single fault with length of 250 km and width of 100 km (black rectangle).

2. THEORY AND METHODOLOGY

2.1 Linear dispersive equations: tsunami in deep water

In Cartesian coordinates the 2-D DSP equations can be written as (Saito *et al.*, 2010)

$$\frac{\partial \eta}{\partial t} = -\left(\frac{\partial M}{\partial x} + \frac{\partial N}{\partial y}\right) \quad (1)$$

$$\frac{\partial M}{\partial t} + gh\frac{\partial \eta}{\partial x} = \frac{1}{3}h^2\frac{\partial^2}{\partial x \partial t}\left(\frac{\partial M}{\partial x} + \frac{\partial N}{\partial y}\right) \quad (2)$$

$$\frac{\partial N}{\partial t} + gh\frac{\partial \eta}{\partial y} = \frac{1}{3}h^2\frac{\partial^2}{\partial y \partial t}\left(\frac{\partial M}{\partial x} + \frac{\partial N}{\partial y}\right) \quad (3)$$

,where M and N are the velocity components (u, v) in x and y direction integrated along the vertical direction from the sea bottom to the sea surface, η is sea surface fluctuation, h is water depth, and g is acceleration due to gravity. The right hand sides of Eq. (2) and Eq. (3) indicate dispersion terms

2.2 Nonlinear long-wave equations: tsunami near shore

For very shallow water or near coast, we need to keep the advection terms and to consider the contribution of bottom friction. The NLLW equations including these effects can be written as (Intergovernmental Oceanographic Commission (IOC), 1997),

$$\frac{\partial \eta}{\partial t} + \frac{\partial M}{\partial x} + \frac{\partial N}{\partial y} = 0 \quad (4)$$

$$\frac{\partial M}{\partial t} + \frac{\partial}{\partial x}\left(\frac{M^2}{D}\right) + \frac{\partial}{\partial y}\left(\frac{MN}{D}\right) + gD\frac{\partial \eta}{\partial x} + \frac{gn^2}{D^{7/3}}M\sqrt{M^2 + N^2} = 0 \quad (5)$$

$$\frac{\partial N}{\partial t}+\frac{\partial}{\partial x}\left(\frac{MN}{D}\right)+\frac{\partial}{\partial y}\left(\frac{N^2}{D}\right)+gD\frac{\partial \eta}{\partial y}+\frac{gn^2}{D^{7/3}}N\sqrt{M^2+N^2}=0 \quad (6)$$

,where $D=h+\eta$ is total water depth. $\frac{gn^2}{D^{7/3}}M\sqrt{M^2+N^2}$ and $\frac{gn^2}{D^{7/3}}N\sqrt{M^2+N^2}$ are the bottom friction terms. n is called Manning's roughness coefficient.

2.3 Linear long-wave equations as conventional equations

The LLW is an approximation of the DSP equations or NLLW equations. If we neglect the right side Eqs. (2) and (3) of the DSP equations or if we neglect the advection and the bottom friction terms, we will obtain the LLW equations.

$$\frac{\partial \eta}{\partial t}=-\left(\frac{\partial M}{\partial x}+\frac{\partial N}{\partial y}\right) \quad (7)$$

$$\frac{\partial M}{\partial t}+gh\frac{\partial \eta}{\partial x}=0 \quad (8)$$

$$\frac{\partial N}{\partial t}+gh\frac{\partial \eta}{\partial y}=0 \quad (9)$$

2.4 Procedure for tsunami simulations

To perform tsunami simulations, the bathymetry data, output points (tide gauge and Ocean Bottom Pressure Gauge (OBPG)) and initial seafloor deformation as tsunami source must be prepared.

The computation area for our simulation is from 95°E-104°E and 6°S-2°N (1620 × 1440). For DSP simulation, we prepared the bathymetry data with a grid size of 999 km × 888 km from the 20 arc-second (dx = 616.6667 m and dy = 616.6667 m) bathymetry data (Satake *et al*., 2012), which was used for estimating the tsunami source of the 2010 Mentawai earthquake. Time step of 1 s were chosen for all simulations considering the Courant-Friedrichs-Lewy (CFL) to avoid numerical instabilities.

3. RESULT AND DISCUSSION

3.1 A future event of Mw 8.5 as a probable scenario

For the future event we assume an earthquake characterized by a single fault with a length of 250 km and width of 100 km around the seismic gap in the the west part of Padang area (Figure 1). Also, we assume that the maximum slip is 9.0 m which is the same as that of the 2007 Bengkulu earthquake (Fujii and Satake, 2008) and the shear modulus (μ) is 2.66 × 10^{10} N/m^2 from the Preliminary Reference Earth Model (PREM) (Dziewonski and Anderson, 1981). These fault parameters would produce an earthquake of magnitude 8.5. Initial seafloor deformation calculated from the earthquake fault model produces maximum uplift of 3.39 m and maximum subsidence of 1.82 m (Figure 2).

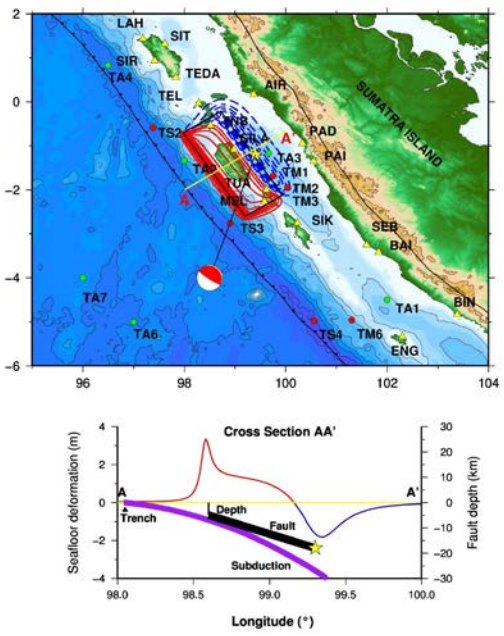

Figure 2. Initial seafloor deformation for a future event of Mw 8.5.

3.1.1 Tsunami propagation in deep water

We can see that dominant dispersive waves appear in a direction perpendicular to the fault strike (Figure 3a). In deep water, the results of the DSP are almost similar with LLW, but for the OBPG TA7 (Figure 3b) the waveform calculated by the DSP simulation is very different from the LLW.

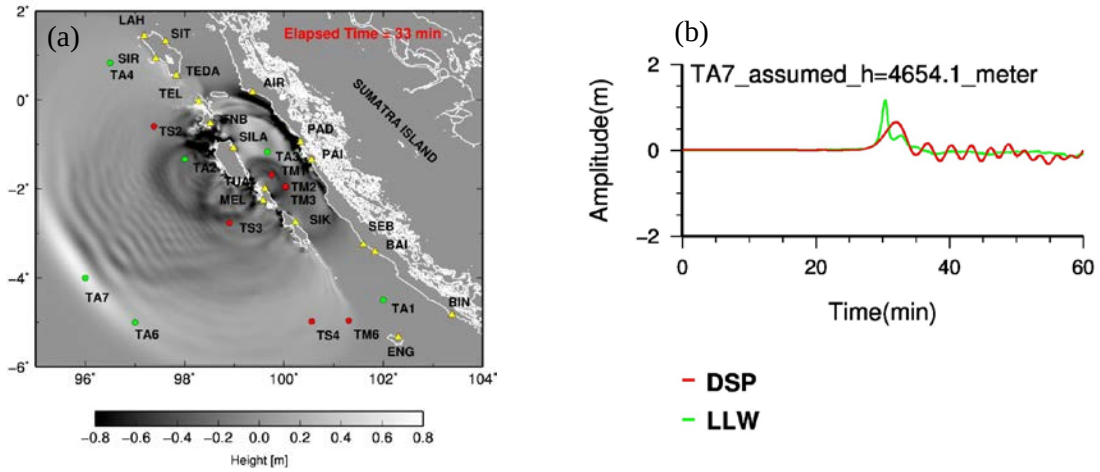

Figure 3. (a) Snapshot of the tsunami wave propagation (t = 33 min) obtained from the DSP simulation. (b) DSP (red line) and LLW (green line) calculated at TA7, a OBPG station assumed in this study, which located at water depth of 4654.1 m.

Dispersive waves dependent on fault depth

DSP simulations for a future event of Mw 8.5 using different fault depths are also conducted. The fault depth becomes deeper to the east, following the subduction zone. Simulated all waveforms for fault depths of 5, 10, and 20 km shows that when the fault depth is shallow, the uplift becomes steep and dispersive wave becomes more dominant at TA7. If the fault depth is deeper the uplift becomes a more gentle slope, and there are no dispersive waves predicted at TA7. This implies that the dispersive wave may be a good measure for judging whether earthquake rupture reaches very shallow part near the trench or the rupture occurs only in deep part.

3.1.2 Tsunami propagation in shallow water

To investigate the contributions of non-linear effects in shallow water, NLLW was compared with LLW. Figure 4 shows the calculated waveform at the Padang tide gauge, together with the simulation results of the LLW equations, which indicates that there is a significant difference between the waveforms of the NLLW and LLW equations. This difference is caused by the advection and bottom friction terms included in the NLLW equations.

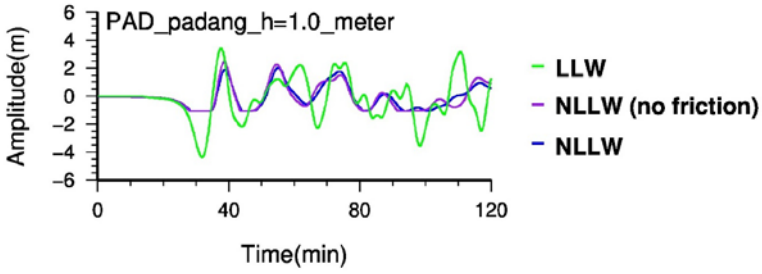

Figure 4. Comparison of tsunami waveforms among LLW, NLLW with no bottom friction and NLLW including advection and bottom friction terms.

Effect of bottom friction in shallow water

In order to examine the effect of bottom friction in shallow water, the results of an NLLW simulation (Mw 8.5) without bottom friction (Manning's roughness coefficient n is set to 0) and those of an NLLW simulation with n = 0.025 are compared (Figure 4). The results of our simulation show that NLLW without bottom friction almost similar with NLLW (e.g. Satake, 1995). In very shallow water areas (h < 10 m) bottom friction becomes important to reduce the tsunami amplitude. But generally if we compare LLW, NLLW without bottom friction, and NLLW (Figure 4), the effect of advection terms are more dominant than the effect of bottom friction.

To find the relationship between linear effects, non-linear effects and sea depth a Normalized Mean Square Residual (NMSR) was calculated. NMSR equations can be written as

$$NMSR = \frac{\sum_{i=1}^{n} |y_L(t_i) - y_N(t_i)|^2}{\sum_{i=1}^{n} |y_N(t_i)|^2} \qquad (10)$$

where y_L and y_N are amplitudes of LLW and of NLLW at time *i*, respectively.

The calculated NMSR (Figure 5) shows that when the sea depth is greater than 50 m, the NMSR value is low, except blue triangle (Tua pejat station), this indicates that for deep water we can use both LLW and NLLW. At the Tua pejat station, which is located at the source, it is difficult to distinguish propagation waves if the station suddenly records a tsunami. For shallow water less than 50 m, NMSR gives scattered results and higher values indicating that we should consider non linear effects in this case.

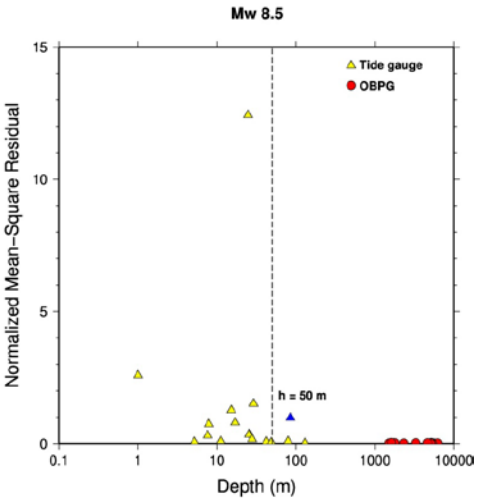

Figure 5. NMSR from the calculated waveforms of LLW and NLLW for the future event of Mw 8.5.

Maximum tsunami height and tsunami arrival time in coastal area

The simulation for a future event of Mw 8.5 resulted maximum heights at Padang station (PAD) (Figure 6a) of 2.02 m using NLLW and 3.40 m using LLW. This tsunami height would be dangerous as Padang is very close to the sea, and also does not have a sea wall to reduce the energy of a tsunami. Tsunami arrival time at PAD is around 20 min (Figure 6b). Our institution (BMKG) gives a tsunami warning 5 min after origin time of earthquake, in this case the people of the Padang area have 15 min to escape to an evacuation area.

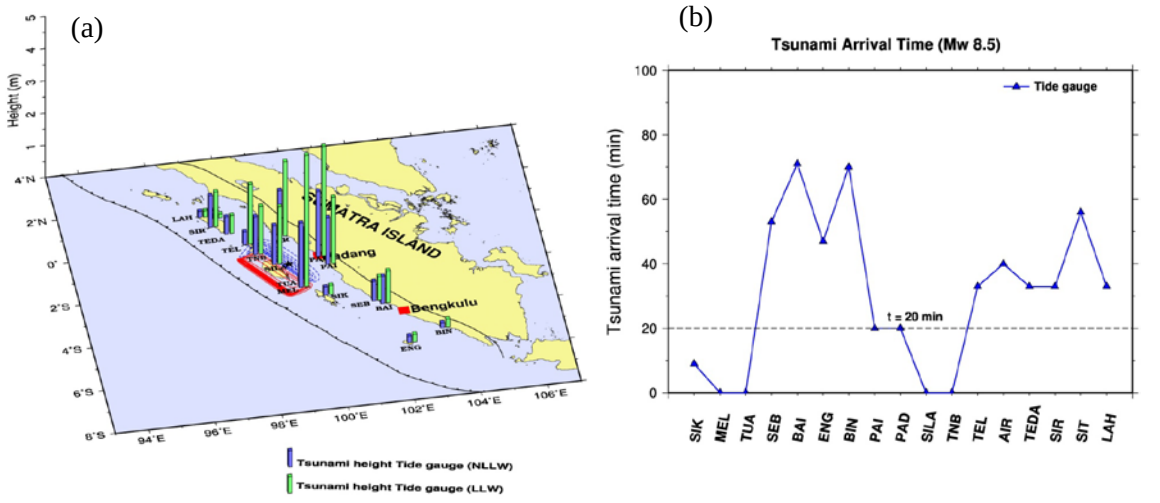

Figure 6. (a) Distribution of maximum tsunami heights at tide gauge stations with comparison of NLLW (blue bars) versus LLW (green bars). (b) Tsunami arrival times at tide gauge stations for a future event of Mw 8.5.

3.2 Future events: large scenario of Mw 8.9 and lower scenario of Mw 8.1

Assuming Mw 8.9 for larger case and Mw 8.1 for smaller case, we evaluate how maximum tsunami height in the Padang area changes. For both scenarios, we assume that the fault length and width are the same as the Mw 8.5 scenario, only the slip amounts are different.

Maximum tsunami height and tsunami arrival time in coastal area

Future events of Mw 8.9 and 8.1 produce the maximum tsunami height at At Padang area is 5.65 m (13.6 m using LLW) and 0.91 m (1.05 m using LLW). Tsunami arrival times in the Padang area are 17 and 24 min for Mw 8.9 and 8.1, respectively. Tsunami arrival times in the Padang area, where first tsunamis are negative waves, shows that tsunami arrival times in all cases are very short. For the preparedness we should make good evacuation maps for communities near the coastal sea.

4. CONCLUSIONS

1. In deep water, DSP equations well agree with LLW. Dispersive waves appear at TA7 which is located perpendicular to the fault strike. We found that dispersive waves depend on fault depth. If the fault depth is shallow, more dispersive waves will appear. Dispersive waves play a significant role to judge the rupture of the earthquake reached to the very shallow part near trench or occured only in deep part.
2. When water depth is shallower than 50 m, the effects of advection terms and bottom frictions should be considered. In shallow water the effect of advection terms are more dominant than the bottom frictions.
3. Simulation results for a future event in the Padang area indicate the maximum heights of 0.9 m, 2.0 m and 5.7 m for the scenarios of Mw of 8.1, 8.5 and 8.9, respectively. The arrival time of the first negative tsunami wave in the Padang area are 24, 20 and 17 min for Mw 8.1, 8.5 and 8.9, respectively.

REFERENCES

Dziewonski, A. M., and D. L. Anderson., 1981, *Phys. Earth Planet. Inter*., 25, 297–356, doi:10.1016/0031- 9201(81)90046-7.

Fujii, Y., and Satake, K., 2008, *Earth Planets Space*, Vol. 60, pp. 993-998.

Intergovermental Oceanographic Commission, 1997, IUGG/IOC Time Project, IOC Manuals and Guides No 35, UNESCO.

Natawidjaja, D. H., Sieh, K., Chlieh, M., Galetzka, J., Suwargadi, B. W., Cheng, H., Edwards, R. L., Avouac, J. P., and Ward, S. N., 2006, *J. Geophys. Res*., Vol. 111, B06403, doi:10.1029/2005JB004025.

Natawidjaja, D. H., 2007, pelatihan pemodelan run-up tsunami, RISTEK.

Newman, A. V., Hayes, G., Wei, Y., and Convers, J., 2011, *Geophys. Res. Lett*, Vol. 38, L05302, doi:10.1029/2010GL046498.

Saito, T., Satake, K., and Furumura, T., 2010, *J. Geophys. Res*, Vol. 115, B06303, doi:10.1029/2009JB006884.

Satake, K., 1995, *PAGEOPH*, Vol. 144, pp. 455-470.

Satake, K., Nishimura, Y., Putra, P. S., Gusman, A. R., Sunendar, H., Fujii, Y., Tanioka, Y., Latief, H., and Yulianto, E., 2012, *PAGEOPH*, doi 10.1007/s00024-012-0536-y.